



Cortical porosity is elevated after a single dose of zoledronate in two rodent models of chronic kidney disease

Elizabeth A. Swallow^a, Corinne E. Metzger^a, Neal X. Chen^b, Joseph M. Wallace^c, Samantha P. Tippen^a, Rachel Kohler^c, Sharon M. Moe^{b,d}, Matthew R. Allen^{a,b,c,d,*}

^a Department of Anatomy, Cell Biology & Physiology, Indiana University School of Medicine, Indianapolis, IN, United States

^b Department of Medicine, Division of Nephrology, Indiana University School of Medicine, Indianapolis, IN, United States

^c Department of Biomedical Engineering, Indiana University Purdue University of Indianapolis, Indianapolis, IN, United States

^d Roudebush Veterans Administration Medical Center, Indianapolis, IN, United States

ARTICLE INFO

Keywords:

Bisphosphonates
Chronic kidney disease (CKD)
Bone
Cortical porosity

ABSTRACT

Purpose: Patients with chronic kidney disease (CKD) have high risk of fracture in part due to cortical bone deterioration. The goal of this study was to assess the impact of two different bisphosphonates and dosing regimens on cortical microstructure (porosity, thickness, area) and bone mechanical properties in animal models of CKD.

Methods: In experiment 1, Male Cy/+ (CKD) rats were treated with either a single dose or ten fractionated doses of zoledronate at 18 weeks of age. Fractionated animals received 1/10th of single dose given weekly for 10 weeks, with study endpoint at 28 weeks of age. In experiment 2, male C57Bl/6 J mice were given dietary adenine (0.2%) to induce CKD. Bisphosphonate treated groups were given either a single dose of zoledronate or weekly risedronate injections for 4 weeks. Cortical microstructure was assessed via μ CT and mechanical parameters evaluated by monotonic bending tests.

Results: Exp 1: CKD rats had higher blood urea nitrogen (BUN) and parathyroid hormone (PTH) compared to NL littermate controls. Single dose zoledronate had significantly higher cortical porosity in CKD S.Zol (2.29%) compared to NL control (0.04%) and untreated CKD (0.14%) ($p = 0.004$). Exp 2: All adenine groups had significantly higher BUN and PTH compared to control mice. Mice treated with single dose zoledronate (Ad + Zol) had the highest porosity (~6%), which was significantly higher compared to either Ad or Ad + Ris (~3%; $p < 0.0001$) and control mice had the lowest cortical porosity (0.35%). In both experiments, mechanics were minimally affected by any bisphosphonate dosing regimen.

Conclusion: A single dose of zoledronate leads to higher cortical porosity compared to more frequent dosing of bisphosphonates (fractionated zoledronate or risedronate). Bisphosphonate treatment demonstrated limited effectiveness in preventing cortical bone microstructure deterioration with mechanical parameters remaining compromised due to CKD and/or secondary hyperparathyroidism irrespective of bisphosphonate treatment.

1. Introduction

One in seven individuals in the United States is estimated to have CKD (Center for Disease Control and Prevention, 2021). These numbers are expected to increase in the coming decade due to an aging population and increased incidence of other diseases linked to CKD prevalence (Center for Disease Control and Prevention, 2021; Bowe et al., 2018). Numerous studies have demonstrated that fracture risk is higher in

individuals with moderate-to-severe CKD compared to the non-CKD population (Nickolas et al., 2006; Nickolas et al., 2008; Moe and Nickolas, 2016; Ensrud et al., 2007; Coco and Rush, 2000; Ball et al., 2002; Alem et al., 2000). Furthermore, secondary effects of fracture, such as fracture-related complications and mortality, are higher in patients with CKD (Coco and Rush, 2000; Tentori et al., 2014). Finding effective treatments that mitigate skeletal fractures in CKD patients would improve both patient care and CKD outcomes.

* Corresponding author at: Dept. of Anatomy and Cell Biology, MS 5035, Indiana University School of Medicine, 635 Barnhill Dr., Indianapolis, IN 46202, United States.

E-mail address: matallen@iu.edu (M.R. Allen).

<https://doi.org/10.1016/j.bonr.2022.101174>

Received 21 December 2021; Received in revised form 4 February 2022; Accepted 5 February 2022

Available online 7 February 2022

2352-1872/Published by Elsevier Inc. This is an open access article under the CC BY-NC-ND license (<http://creativecommons.org/licenses/by-nc-nd/4.0/>).

Bisphosphonates are an effective pharmacological intervention that reduce skeletal fragility in various conditions including postmenopausal osteoporosis (Burr and Allen, 2012; Eastell et al., 2011). Few clinical studies have undertaken specific investigation of bisphosphonates in advanced CKD patients, and their current use in patients with an estimated glomerular filtration rate <30 mL/min/m² (Grade/Stage 4 or 5) is not recommended by the FDA due to concerns of accumulation and impaired renal clearance of the drug that may cause unwanted bone effects. However, the limited small trials and secondary analyses suggests potential benefit to bone and with changing clinical guidelines permitting bisphosphonate use in CKD patients by the Kidney Disease Improving Global Outcomes (KDIGO) committee, understanding whether these agents are effective in mitigating bone loss is important for patient health (Wilson et al., 2017; Toussaint et al., 2010; Bergner et al., 2008; Ketteler et al., 2017).

Several pre-clinical studies have explored bisphosphonate use and their effects on the skeleton. Our lab has previously documented the efficacy of a single dose of zoledronate in suppressing elevated bone remodeling without producing adynamic bone (Allen et al., 2013). We have also documented that while there are higher levels of drug accumulation in the skeleton of CKD animals compared to healthy controls, weekly administrations (fractionating) to achieve the same cumulative dose resulted in significantly lower skeletal accumulation (Swallow et al., 2018; Swallow et al., 2019). Whether or not dosing bisphosphonates in a fractionated manner alters CKD-induced changes in cortical bone microstructure and mechanical integrity relative to single dose is unknown.

Herein we report the results of two independent experiments that were both focused on determining the impact of dosing regimens of bisphosphonates on cortical microstructure and mechanical properties in the setting of CKD. In experiment 1, rats with progressive kidney disease were treated with either a single dose or a weekly fractionated dose of zoledronate over a period of 10-weeks. We hypothesized fractionated dosing, due to the lower accumulation as shown in previous studies, would provide greater protection from CKD cortical bone deterioration than a single dose of zoledronate. In Experiment 2, we compared two different bisphosphonates using clinically relevant dosing

regimens (single zoledronate dose versus multiple risedronate doses) in a mouse adenine model to test the hypothesis that clinically relevant doses that are administered more frequently are superior in preserving cortical microstructure and mechanical properties compared to less frequent regimens, again based on assumptions around skeletal accumulation, in the setting of CKD.

2. Methods

All experiments were approved prior to their initiation by the Indiana University School of Medicine Institutional Animal Care and Use Committee.

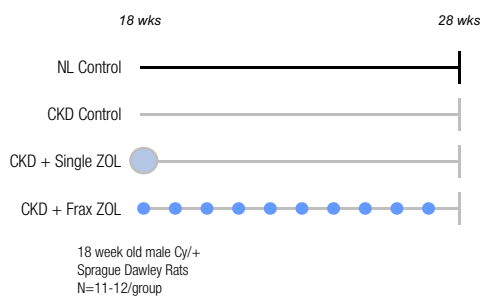
2.1. Experiment 1

2.1.1. Animal model and experimental design

Male Cy/+ Sprague Dawley (Han:SPRD) rats, a model of high turnover CKD (Allen et al., 2013; Moe et al., 2014), from an in-house breeding colony were screened at 10 weeks of age for elevated circulating blood urea nitrogen (BUN) as a biomarker of reduced kidney function (Moe et al., 2011). Animals were identified and categorized as either CKD or normal unaffected healthy littermate controls (NL). From 10 weeks of age on, rats were singly housed in a room with 12-h light/dark cycles and an average temperature of 70 °F. At 17 weeks of age, all animals were switched from the facility-provided grain-based diet to a casein-based diet with adjusted calcium and phosphorus ratio, 0.6% and 0.9% respectively, (Harlan Teklad TD.04539), which we have shown supports CKD progression (Moe et al., 2009). Food and water were provided ad libitum for the duration of the study. At 18 weeks of age, animals were randomly assigned to one of the following groups (Fig. 1):

1. NL – normal littermate controls, no treatment
2. CKD – no treatment
3. CKD S.Zol – single bolus dose of zoledronate
4. CKD F.Zol – fractionated zoledronate (1/10th of single dose given weekly for 10 weeks).

Experiment 1



Experiment 2

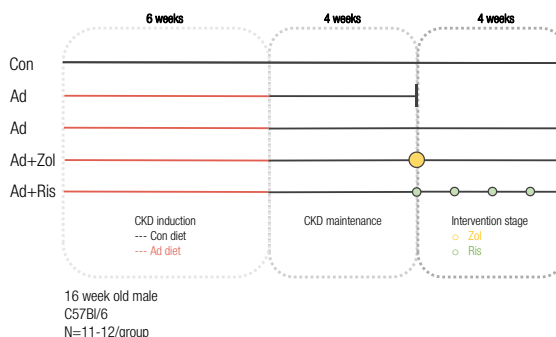


Fig. 1. A schematic of the experimental designs. Experiment 1: rat model, shows group assignments based on disease state NL (black lines) and CKD (grey lines). Treatment begun at 18 weeks of age. The light blue dot represents a single dose of zoledronate (Zol) whereas, multiple smaller dark blue dots represent Zol fractionation. Experiment 2: mouse model, shows the 3 stages of the experiment (grey dotted rectangles). The period of CKD induction (red line) for Ad groups relates to the administration of adenine diet. Bisphosphonate treatment is displayed by a large yellow dot (single dose) ZOL or smaller green dots that signify weekly risedronate (Ris) administration.

Animals in the single dose zoledronate group (S.Zol) received a single subcutaneous dose (20 $\mu\text{g}/\text{kg}$) at 18 weeks of age (Moe et al., 2014). This dose was shown to effectively suppress remodeling in this animal model of CKD. Animals in the fractionated zoledronate group (F.Zol) received a weekly subcutaneous dose of 2 $\mu\text{g}/\text{kg}$. Each group had 12 rats/group except for CKD S.Zol that had 11/group at endpoint because one rat was found dead (unknown cause) at 24 weeks of age. At 28 weeks of age, all animals were anesthetized under vaporized isoflurane and euthanized via thoracotomy and tissues were collected.

2.1.2. Biochemistries

Blood was collected by tail bleed prior to euthanasia. Capillary tubes were centrifuged to collect plasma (~ 200 μL) and then immediately frozen for biochemistry assays. Blood urea nitrogen (BUN) was analyzed by colorimetric assay (BioAssay Systems, Hayward, CA) and intact parathyroid hormone (iPTH) was measured by ELISA (Immutopics, San Clemente, CA) as previously described (Swallow et al., 2019; Moe et al., 2014; Mecnery et al., 2019).

2.1.3. Micro-computed tomography (μCT)

Left femurs (distal two thirds) were scanned individually on a SkyScan 1176 (Bruker, Billerica, MA, USA) at 9 μm voxel size with 0.5 aluminum filter, 2 frame averaging, and 0.7 rotation step. Cortical geometry and microstructure parameters were measured from two slices from the femoral mid-shaft (50% total bone length). A single investigator manually drew a region of interest (ROI) that traced the endocortical and periosteal surfaces of bone to isolate only the cortical bone. Cortical porosity (Ct.Po, %) was defined as the void area between the periosteal and endocortical surfaces and a single value represented an average of the two slices for each animal based on data from a small cohort of animals where we studied assessment of 1–5 slices. Cortical thickness, cortical bone area, and cross sectional moment of inertia (CSMI) were calculated using manufacturer software (CtAN, Bruker) (Bouxsein et al., 2010).

2.1.4. 3-pt bending monotonic mechanical test

At the time of mechanical testing, femurs were thawed at room temperature (from storage in saline-soaked gauze at -20 $^{\circ}\text{C}$) and remained soaked in saline until mechanical testing. Bones were measured for total length and anterior-posterior (AP) diameter using callipers. Bones were tested to failure using a mechanical testing system (Test Resources, Shakopee, MN, USA) in 3-pt bending (lower support span 18 mm). A 667.2 N load cell and a 2 mm/min displacement rate were used for all tests. Bones were oriented with the anterior surface of the femur in compression with the loading point at 50% bone length. All bones were pre-loaded with 0.5 N and kept hydrated before beginning the tests. Moment of inertia was obtained from CtAN (Bruker, see above μCT methods) and used to estimate material level properties using standardized bending eqs. A custom MATLAB script, using force-displacement data and cortical geometry values as inputs, was used to determine structural and estimated material level properties (Allen et al., 2013; Moe et al., 2014; Fuchs et al., 2008). Reported measures presented follow standard nomenclature (Turner and Burr, 1993).

2.1.5. Statistical analysis

All data was analyzed in IBM SPSS Statistics 26 (IBM, Armonk, NY, USA) and graphed in Prism 7.03 (Graphpad, San Diego, CA). Data were tested for normality and homoscedasticity via Shapiro-Wilk tests. If parameters failed normality or homoscedasticity testing then, data were run by a Kruskal-Wallis (non-parametric ANOVA) test. Due to this, PTH, cortical porosity, cortical thickness, displacement to yield, and work to yield were analyzed by Kruskal-Wallis tests. When p -values reached statistical significance ($p < 0.05$), pairwise comparisons with Bonferroni corrections were performed to account for multiple tests and to identify groups that differed. Non-parametric data is presented as median [range]. The remaining parameters that passed normality tests were

analyzed via a one-way ANOVA. If the ANOVA reached statistical significance ($p < 0.05$), Tukey tests were performed for post hoc comparisons. Data is presented as mean \pm standard deviation (SD). Alphabetical notation is used to display post hoc analysis. Groups that do not share the same letter are statistically different from each other.

2.2. Experiment 2

2.2.1. Animal model and experimental design

Male C57Bl/6 J mice ($n = 12$ per group) were ordered from Jackson Laboratories (Bar Harbor, ME, USA) at 15 weeks of age. Mice were group housed in an institutionally approved facility with 12-h light/dark cycle and an average temperature of 70 $^{\circ}\text{F}$. Mice were given a week to acclimatize to the facility and were randomly assigned to one of the following groups (Fig. 1):

1. Adenine baseline (10-week)
2. Control
3. Adenine
4. Adenine + Zoledronate (Ad + Zol)
5. Adenine + Risedronate (Ad + Ris)

At 16 weeks of age, all mice were switched to a purified casein-based diet with adjusted calcium and phosphorus (0.6% Ca, 0.9% P). Animals designated to adenine (CKD) groups were fed the same adjusted casein diet with the addition of 0.2% adenine (Envigo Teklad Diets, Madison, WI, USA). The adenine mouse model has been previously characterized as a model of high turnover CKD (Metzger et al., 2021a; Metzger et al., 2021b). Mice were placed on the adenine diet for 6 weeks for a phase of disease initiation before being switched back to the control casein-based diet for 4 weeks for a period of maintenance (Metzger et al., 2021b; Metzger et al., 2020b). A group ($n = 12$) of adenine baseline mice was euthanized at this 10-week point. For the remaining mice, the intervention stage (4 weeks) began at 26 weeks of age. The Ad + Zol group was given a single subcutaneous dose of zoledronate (60 $\mu\text{g}/\text{kg}$) at 26 weeks of age while the Ad + Ris group was given weekly subcutaneous injections of risedronate (3.5 $\mu\text{g}/\text{kg}$) for 4 weeks (Fig. 1.) (Allen et al., 2011). These doses correspond, on a mg/kg basis, to clinically-relevant doses and have been shown to have skeletal effects in wild-type mice (Aref et al., 2016). Mice were monitored regularly, and body weight was tracked weekly throughout the study. All mice made it to study endpoint except for one Ad + Zol mouse that was euthanized during the maintenance phase due to low body conditioning score and declining body weight. At study endpoints (10 weeks for adenine baseline group or 14 weeks for all others), animals were anesthetized via vaporized inhaled isoflurane and euthanized via exsanguination and thoracotomy after which tissues were collected.

2.2.2. Biochemistries

Blood was collected (~ 1 mL) at study endpoint under isoflurane anesthesia via cardiac stick. Blood was centrifuged, and serum was immediately frozen for future biochemistry assays. BUN and intact PTH was measured by ELISA (Immutopics, San Clemente, CA) as previously described (Metzger et al., 2021a, 2021b; Metzger et al., 2020a, 2020b).

2.2.3. Micro-computed tomography (μCT)

Right distal femurs were scanned on a SkyScan 1172 (Bruker, Billerica, MA, USA) at 8 μm voxel size with 0.5 aluminum filter, 2 frame averaging, and 0.7 rotation step. Cortical geometry and microstructure parameters were measured ~ 3 –4 mm proximally to the distal femur growth plate. Analyses were done as described in Experiment 1 except for the additional secondary analysis of pore number. This parameter utilized inverse thresholding to make pores appear white and CtAN trabecular functions were applied to analyze pore number.

For assessment of mechanics, right tibiae were scanned for mechanics testing as previously described in a custom holder for 3 bones

per scan on a Skyscan 1172 (Bruker Billerica, MA, USA) with a voxel size of 17 μm , 0.7 rotation step, no frame averaging, and 0.5 Al filter to obtain geometric properties (moment of inertia about the bending axis and distance from the centroid to the bone surface) in the region of testing (Kohler et al., 2021). Scans were reconstructed and rotated before 10 slices were selected near the midpoint of the testing region. This volume was then run through a custom MATLAB code as previously described (Berman et al., 2015).

2.2.4. 4-pt bending monotonic mechanical tests

At the time of mechanical testing, tibiae were thawed at room temperature and remained soaked in saline until mechanical testing. Bones were tested to failure using a mechanical testing system (Bose Electro-Force 5500; TA Instruments, New Castle, DE, USA) with a 43.9 N load cell in 4-pt bending with a bottom support span of 8 mm and a top loading span of 3 mm. Bones were tested in the medial-lateral direction with the medial surface in tension. All bones were pre-loaded with 0.5 N, tested with a displacement rate of 0.025 mm/s, and kept hydrated before beginning the tests (Wallace et al., 2009). A custom MATLAB script, using force-displacement data and cortical geometry values, was used to determine structural-level and estimate material-level properties (Allen et al., 2013; Moe et al., 2014; Fuchs et al., 2008). Reported measures presented followed standard nomenclature (Turner and Burr, 1993).

2.2.5. Immunohistochemistry

Fixed left femurs were decalcified in 14% EDTA (~2 weeks) and embedded in paraffin. Serial longitudinal 5 μm sections were taken and stained using an avidin-biotin method. Samples were stained for receptor activator of nuclear factor κB ligand (RANKL; Abcam, Cambridge, MA, USA) and annexin V (Abcam), an early marker of cellular apoptosis. Counterstaining and negative controls for all antibodies were conducted using methods as previously described (Metzger et al., 2021a; Metzger et al., 2020a). Sections were analyzed in a standard ROI in the cortical bone of the femur midshaft. Results were reported as the percentage of osteocytes stained positively for the protein out of all osteocytes within the ROI. All analyses were completed by the same blinded investigator.

2.2.6. Statistical analysis

All data was analyzed in IBM SPSS Statistics 26 (IBM, Armonk, NY, USA) and graphed in Prism 7.03 (Graphpad, San Diego, CA). To determine the impacts of time on CKD progression, a *t*-test was performed between 10-week adenine (baseline) and 14-week adenine (endpoint) mice except for PTH which failed a Shapiro-Wilk normality test, so a non-parametric *t*-test was performed. Study endpoint parameters were tested for normality and homoscedascity via Shapiro-Wilk tests. If parameters failed normality or homoscedascity testing then, data were run by a Kruskal-Wallis (non-parametric ANOVA) test. Cortical porosity, PTH, cross-sectional moment of inertia (CSMI), ultimate force, displacement to yield, post-yield displacement, total displacement, post-yield work, total work, total strain, and toughness were all analyzed by Kruskal-Wallis tests. Pairwise comparisons were performed with Bonferroni corrections to identify groups that differed when appropriate ($p < 0.05$). All non-parametric data is presented as medium [range]. All other remaining parameters were compared via a one-way ANOVA with a statistical significance threshold set at $p < 0.05$. If parameters reached significance, then a Tukey's test for post hoc analysis was performed to assess individual group differences ($p < 0.05$). Data is presented as mean \pm SD. Alphabetical notation is used to display post hoc analysis. Groups that do not share the same letter are statistically different from each other.

3. Results

3.1. Experiment 1

3.1.1. Biochemistries

At 28 weeks of age, all CKD groups had 2-fold higher BUN values compared to normal littermates, confirming CKD (ANOVA $p < 0.0001$, Table 1). Neither zoledronate treatment regimen (single or fractionated dosing) affected BUN compared to untreated CKD rats. PTH was approximately 5- and 9-fold higher in CKD control and CKD S.Zol, respectively, compared to NL control (ANOVA $p = 0.001$, Table 1). PTH values in the CKD F.Zol group did not differ from normal controls or any other CKD groups (CKD control or single dose ZOL) (Table 1).

3.1.2. Cortical microstructure

Cortical bone area was lower in untreated CKD compared to NL control and CKD F.Zol (-4 and -7%, respectively; ANOVA $p = 0.006$, Fig. 2A). Cortical bone area for CKD S.Zol did not differ from any other group. Cortical thickness was not different among groups (ANOVA $p = 0.07$, Fig. 2B). Cortical porosity was significantly higher in CKD S.Zol (2.29%) compared to NL control (0.04%) and untreated CKD (0.14%) (ANOVA $p = 0.004$, Fig. 2C). Cortical porosity in CKD F.Zol group (0.62%) did not differ from any other CKD group (Fig. 2C, D).

3.1.3. Structural- and material-level mechanical parameters

The structural mechanical parameter of stiffness was significantly lower in CKD control and CKD S.Zol groups compared to NL (ANOVA $p < 0.0001$, Fig. 2E). CKD F.Zol had significantly higher stiffness compared to untreated CKD but did not differ from CKD S.Zol. Ultimate force was significantly lower in both CKD control and CKD S.Zol compared to NL control (ANOVA $p = 0.003$, Fig. 2F). CKD F.Zol did not differ from any other group for ultimate force (Fig. 2F). When adjusted for geometry, the estimated material mechanical parameters of modulus and ultimate stress were no different between groups (ANOVA $p = 0.079$ and $p = 0.356$ respectively, Fig. 2G, H). The remaining mechanical parameters of post-yield displacement, total displacement, post-yield work, total work, total strain, and toughness showed that all CKD groups were lower than NL controls (Table 1). Cross-sectional moment of inertia also did not differ between groups (Table 1).

3.2. Experiment 2

3.2.1. Comparison of baseline to endpoint adenine mice

14-wk adenine mice had higher body weight at study endpoint compared to 10-wk adenine baseline (10-wks) when bisphosphonate treatment began (*t*-test $p = 0.01$, Table S1). For serum BUN and PTH, there were no differences between the two timepoints. Likewise, cortical porosity was not different between the two timepoints (Table S1). Cortical area and cortical thickness were higher (*t*-test $p < 0.001$ and $p = 0.001$, respectively) in the 14-wk mice compared to 10-wk mice (Table S1). Overall, these two groups indicate stable, but not progressive kidney disease and cortical porosity during the intervention phase in this study.

3.2.2. Body weight and biochemistries

All adenine groups had significantly lower body weight compared to the control group irrespective of treatment (ANOVA $p < 0.0001$, Table 2). Additionally, all adenine mice had higher serum BUN compared to control (ANOVA $p < 0.0001$, Table 2). The Ad + Zol group had significantly higher BUN levels compared Ad + Ris (+19%). Whereas adenine alone was no different to either bisphosphonate treated adenine groups. PTH was 3–5-fold higher in all adenine groups compared to control with no differences due to treatment in the adenine groups (ANOVA $p < 0.0001$, Table 2).

Table 1

Experiment 1 (Rat): BUN, PTH, CSMI, and additional structural- and material-level mechanical properties.

	NL control	CKD control	CKD single Zol	CKD Frax Zol	Overall ANOVA P-value
BUN (mg/dL)	19.4 ± 1.9 ^b	49.2 ± 4.7 ^a	50.3 ± 6.1 ^a	47.6 ± 6.9 ^a	<0.0001
PTH (pg/mL)	253.3 [110–971.6] ^b	1226 [561.9–3240] ^a	1504 [340–9770] ^a	444.9 [233.3–1405] ^{ab}	0.001
Cross-sectional moment of inertia (CSMI, mm ⁴)	10.29 ± 0.83	9.68 ± 0.90	9.41 ± 0.96	9.73 ± 0.89	0.138
Displacement to yield (μm)	332.9 [288.2–381.2]	358.8 [312.0–434.1]	347.5 [310.5–405.3]	353.7 [310.2–400.0]	0.250
Post-yield Displacement (μm)	552.6 ± 83.1 ^a	397.1 ± 55.9 ^b	378.5 ± 134.3 ^b	401.1 ± 78.9 ^b	<0.0001
Total Displacement (μm)	889.8 ± 80.6 ^a	755.7 ± 65.0 ^b	733.3 ± 136.2 ^b	758.8 ± 79.6 ^b	0.001
Work to Yield (mJ)	17.71 [14.39–22.99]	18.56 [14.63–29.66]	18.95 [14.18–22.35]	19.24 [16.08–24.11]	0.365
Post-yield Work (mJ)	76.12 ± 12.64 ^a	49.92 ± 10.32 ^b	47.28 ± 18.08 ^b	53.01 ± 12.07 ^b	<0.0001
Total Work (mJ)	94.41 ± 12.85 ^a	69.43 ± 12.70 ^b	66.01 ± 18.30 ^b	72.58 ± 12.58 ^b	<0.0001
Total Strain (ε)	0.060 ± 0.006 ^a	0.049 ± 0.005 ^b	0.047 ± 0.008 ^b	0.048 ± 0.005 ^b	<0.0001
Toughness (MPa)	5.11 ± 0.54 ^a	3.77 ± 0.62 ^b	3.55 ± 0.94 ^b	3.67 ± 0.52 ^b	<0.0001

Data represented as mean ± standard deviation except for PTH, displacement to yield, and work to yield which are displayed as medium [range]. Overall ANOVA p-values are displayed and post-hoc analysis results are marked when appropriate using alphabetical notation. Groups not sharing the same letter are statistically different from each other.

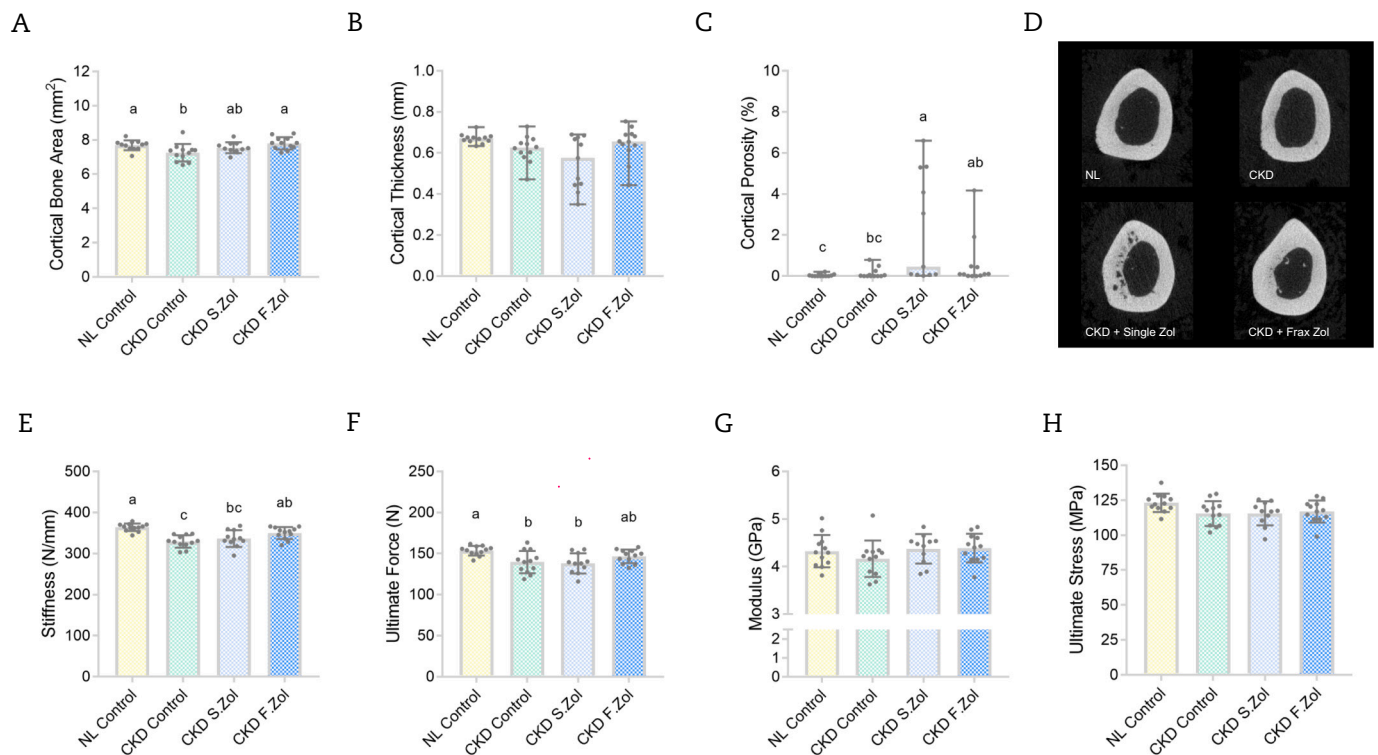


Fig. 2. Cortical microstructure and mechanical parameters in the Cy/+ rat. A) Cortical bone area (Ct. At, mm²) was statistically lower in Ad mice compared to NL control and CKD F.Zol. B) Cortical thickness displayed no difference between groups (Ct.Th, mm). C) Cortical porosity (Ct.Po, %) was significantly higher in CKD S. Zol compared to CKD alone and NL. D) Representative cortical bone images. E) Stiffness (N/mm) is significantly lower in CKD control compared to NL and CKD F.Zol. F) Ultimate force (N) was significantly lower in CKD control and CKD S.Zol compared to NL control. G) Modulus was not different between groups ($p = 0.356$). H) Ultimate stress was not different between groups ($p = 0.079$). Data in Fig. 2A and E-H are displayed as mean ± standard deviation. Data in Figs. 2B & 2C are displayed as median [range]. Graphs display post-hoc analysis when appropriate with statistical difference notated through alphabetical notation. Groups not sharing the same letter are statistically different from each other at $p < 0.05$, $n = 11-12$; see methods.

Table 2

Experiment 2 (mouse) – body weight and biochemistries.

	Control	Ad	Ad + Zol	Ad + Ris	Overall ANOVA P-value
Body weight (g)	34.2 ± 4.1 ^a	26.3 ± 1.8 ^b	25.3 ± 1.4 ^b	25.2 ± 1.2 ^b	<0.0001
BUN (mg/dL)	31.4 ± 5.7 ^c	65.7 ± 10.1 ^{ab}	74.6 ± 13.4 ^a	62.5 ± 11.1 ^b	<0.0001
PTH (pg/mL)	228 [37–314]	898 [496–1594]	747 [509–1139]	727 [219–1973]	<0.0001

Data represented as mean ± standard deviation except for PTH which is displayed as medium [range]. Overall ANOVA p-values are displayed and post-hoc analysis results are marked using alphabetical notation. Groups not sharing the same letter are statistically different from each other.

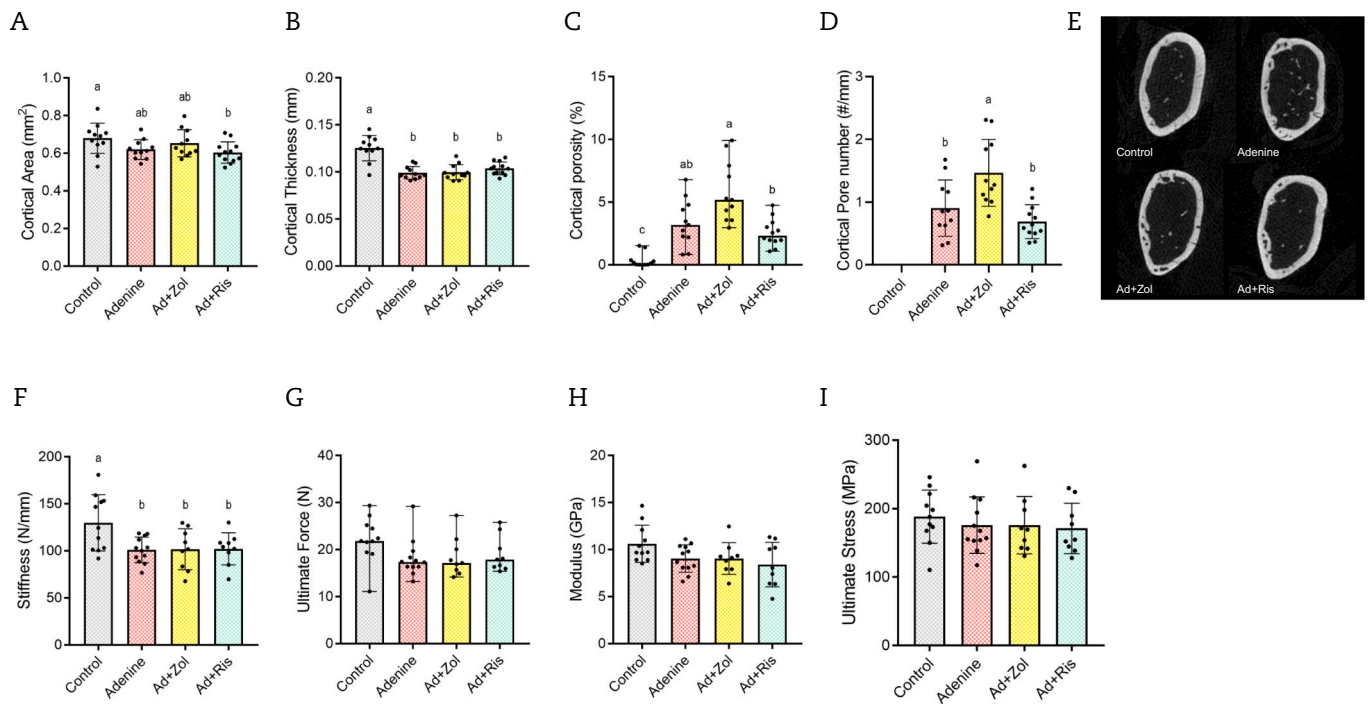


Fig. 3. Cortical microstructure and mechanical parameters in adenine mice. A) Cortical bone area (Ct.Ar, mm²) was significantly lower in Ad alone and Ad + Ris compared to healthy controls. B) Cortical thickness (Ct. Th, mm) was significantly lower in all adenine groups, irrespective of treatment, compared to control. C) Cortical Porosity (Ct.Po, %) was significantly higher in Ad + Zol compared to Ad alone or Ad + Ris. D) Cortical pore number (#/mm) was significantly higher in Ad + Zol compared to Ad alone or Ad + Ris. E) Representative image of cortical bone for each group. F) Stiffness (N/mm) was significantly lower in all adenine groups compared to control. G) Ultimate Force (N) was not different between groups ($p = 0.066$). H) Modulus was no different between groups ($p = 0.066$). I) Ultimate stress was no different between groups ($p = 0.788$). Data in Figs. 3A-3B, 3D, 3F, 3H-3I are displayed as mean \pm standard deviation. Data in Figs. 3C & 3G are displayed as median [range]. Graphs display post-hoc analysis when appropriate with statistical difference notated through alphabetical notation. Groups not sharing the same letter are statistically different from each other at $p < 0.05$, $n = 12$; see methods.

3.2.3. Cortical microstructure

Ad + Ris had lower cortical area compared to control mice (ANOVA $p = 0.043$), while Ad + Zol and adenine was not different from any other group (Fig. 3A). At study endpoint, all adenine groups had significantly lower cortical thickness compared to control (ANOVA $p < 0.0001$, Fig. 3B). As expected, control mice had the lowest cortical porosity (0.35%) with all endpoint adenine groups displaying significantly higher cortical porosity (ANOVA $p < 0.0001$; Fig. 3C, E). Mice treated with single dose zoledronate (Ad + Zol) had the highest porosity (~6%), which was significantly higher compared to Ad + Ris (~3%). Untreated adenine did not differ compared to either bisphosphonate treatment groups (Fig. 3C). Secondary analysis of cortical pore number displayed similar patterns as seen with overall cortical porosity (ANOVA $p < 0.0001$, Fig. 3D). Ad + Zol mice had ~50% higher pore number compared to adenine alone or Ad + Ris (Fig. 3D).

3.2.4. Structural- and material-level mechanical parameters

Adenine mice, irrespective of treatment group, had lower stiffness compared to control (ANOVA $p = 0.008$, Fig. 3F) while ultimate force did not differ between any group (ANOVA $p = 0.066$, Fig. 3G). When adjusting for geometry, the estimated material mechanical parameters of modulus and ultimate stress did not differ between groups (ANOVA $p = 0.066$ and $p = 0.788$ respectively, Fig. 3H, I). The remaining structural and estimated material mechanical parameters as well as cross-sectional moment of inertia did not differ between groups (Table 3).

3.2.5. Immunohistochemistry (IHC)

There were no differences in Annexin V positively-stained osteocytes within the femoral cortical diaphysis at study endpoint (Table 3). The number of RANKL+ osteocytes was significantly higher in CKD groups, with and without bisphosphonate treatment, compared to control mice

Table 3

Experiment 2 (mouse) – immunohistochemistry, CSMI, and additional structural- and material-level mechanical properties.

	Control	Ad	Ad + Zol	Ad + Ris	Overall ANOVA P-value
Annexin V+ (%)	35.9 \pm 10.5	35.9 \pm 10.8	37.4 \pm 7.2	40.7 \pm 5.7	0.639
RANKL+ (%)	18.1 \pm 4.4 ^c	33.4 \pm 7.0 ^b	47.8 \pm 8.4 ^a	42.7 \pm 4.3 ^{ab}	<0.0001
Cross sectional moment of inertia (CSMI, mm ⁴)	0.087 [0.075–0.114]	0.084 [0.075–0.094]	0.079 [0.057–0.104]	0.086 [0.070–0.113]	0.662
Displacement to yield (μ m)	172.3 [121.9–231.5]	162.2 [107.0–238.1]	155.9 [140.5–223.3]	154.1 [94.3–184.4]	0.483
Post-yield Displacement (μ m)	109 [0–632]	180 [2–525]	80 [0–207]	60 [0–587]	0.457
Total displacement (μ m)	257.9 [165.6–812.7]	331.1 [183.9–638.2]	248.3 [142.0–430.3]	244.4 [154.1–717.7]	0.304
Work to yield (mJ)	1.91 \pm 0.66	1.51 \pm 0.87	1.45 \pm 0.56	1.15 \pm 0.59	0.131
Post-yield work (mJ)	1.32 [0.73–9.37]	2.56 [0.04–7.70]	1.15 [0–4.97]	1.40 [0–11.80]	0.516
Total work (mJ)	3.48 [2.04–11.48]	4.05 [1.63–10.88]	2.48 [1.09–6.92]	2.09 [1.29–12.70]	0.402
Total strain (ϵ)	0.027 [0.018–0.083]	0.038 [0.021–0.070]	0.026 [0.015–0.042]	0.27 [0.017–0.084]	0.383
Toughness (MPa)	3.03 [1.51–10.86]	4.44 [1.66–10.65]	2.40 [1.18–5.91]	2.42 [1.26–12.93]	0.341

Data represented as mean \pm standard deviation if normally distributed. Non-parametric data is presented as median [range]. Overall ANOVA p-values are displayed and when appropriate post-hoc analysis results are marked using alphabetical notation. Groups not sharing the same letter are statistically different from each other.

(ANOVA $p < 0.0001$, Table 3). Ad + Zol had significantly higher RANKL positively-stained osteocytes compared to adenine whereas, Ad-Ris was not different from adenine alone or Ad + Zol (Table 3).

4. Discussion

The goal of this study was to assess the impact of two different bisphosphonates and two dosing regimens on cortical microstructure and bone mechanical properties using two different animal models of CKD. We found that a single dose of zoledronate resulted in higher cortical porosity and no apparent mechanical benefit to bone in both a progressive CKD rat model and an adenine-induced mouse model. Additionally, in both models we observed no differences from controls in cortical porosity with bisphosphonate treatment dosed more frequently (Exp.1 – fractionated zoledronate or Exp 2 – weekly risedronate). In both models, bisphosphonate treatments had little to no effect on cortical bone structure or mechanical properties compared to untreated CKD animals, but all CKD animals, regardless of treatment had alterations in cortical bone vs. age-matched controls.

Our approach in this work was to assess concepts of bisphosphonate dosing using two different methodologies (animal models and drug doses). Consistent with previous work (Moe et al., 2014; Moe et al., 2009; McNerny et al., 2019; Metzger et al., 2021b; Metzger et al., 2020a), CKD animals in these two models displayed high PTH and cortical bone deterioration which are consistent with clinical manifestations associated with CKD-mineral bone disorder (CKD-MBD). In this study, cortical deterioration was more pronounced in adenine mice which had both cortical thinning and cortical porosity. These characteristics of bone deterioration were not seen in the Cy rats, likely due to them being at a stage of disease progression prior the significant development of cortical porosity (McNerny et al., 2019).

Bisphosphonates are effective in reducing fracture risk in conditions such as post-menopausal osteoporosis (Burr and Allen, 2012; Eastell et al., 2011; Burr, 2020), yet few clinical studies have studied the effects of bisphosphonates in CKD patients. The importance of reducing fracture risk in the CKD population is critical, since individuals with end-stage renal disease (ESRD) have 60% mortality rate 1 year post hip-fracture compared to 20% mortality rate in the general population (Coco and Rush, 2000). As anti-resorptive agents, bisphosphonates bind to hydroxyapatite and inhibit the activity of osteoclasts impeding bone resorption (Russell et al., 2008). Ideally, mitigation of resorption leads to maintenance of bone mass, improvement in bone mineral density (BMD), and preservation of microstructure. Together these can improve mechanical properties of bone and thus reduce fracture risk (Burr, 2020; Pazianas et al., 2014). The understanding of how bisphosphonates function in the setting of CKD is limited and, due to concerns with renal clearance and renal toxicity, bisphosphonates are not recommended for patients in CKD stages 4 and 5 (eGFR < 30 mL/min/m²). Therefore, animal models can provide a useful surrogate for investigating the impacts of bisphosphonates in CKD and assessing parameters such as whole bone mechanics that cannot be assessed clinically. Our previous work has investigated skeletal accumulation of bisphosphonates and we have shown using a fluorescently tagged-zoledronate (Fam-ZOL; not biologically active) that drug accumulates more in the skeleton of CKD rats than rats with normal kidney function at the same dose (Swallow et al., 2018; Swallow et al., 2019). However, when Fam-ZOL was dosed in a fractionated pattern with smaller and more frequent doses of bisphosphonate, there was lower skeletal accumulation in both healthy and CKD rats (Swallow et al., 2019). Studies have shown that bisphosphonates are effective in suppressing high turnover associated with CKD (Allen et al., 2013; Moe et al., 2014; Newman et al., 2014; Lomashvili et al., 2009; Jokihara et al., 2008); however, few pre-clinical studies in CKD have shown that a single bisphosphonate dose successfully prevents cortical bone loss or improves mechanical parameters. This study goes beyond bisphosphonate skeleton accumulation and asks the question of whether alternative dosing patterns,

smaller and more frequent doses, can be beneficial to CKD bone, both architecturally and mechanically.

In both experimental models, CKD animals treated with a single dose of zoledronate had higher cortical porosity compared to untreated CKD animals. Fractionating zoledronate (in experiment 1) preserved cortical bone area and improved stiffness compared to CKD control animals (Fig. 2). Risedronate dosing at weekly intervals, in experiment 2, is a more realistic clinical approach than fractionating zoledronate; however, cortical microstructure and mechanical parameters remained compromised in adenine mice to a similar degree as a single dose of zoledronate (Fig. 3). Therefore, our study fails to demonstrate a positive impact of bisphosphonates on cortical microstructure and mechanical properties in CKD and brings to light a potential negative outcome with higher cortical porosity with a single dose of zoledronate. Interestingly, despite widespread cortical porosity, a known detrimental factor to the mechanical integrity of bone (Schaffler and Burr, 1988), groups with a single dose of zoledronate, were not significantly affected in mechanical properties beyond disease alone. This builds on two previous papers from our group looking at how bisphosphonates (zoledronate) affect mechanical properties. In our first short term experiment (5 week treatment) we saw modest positive effects on select mechanical properties while our follow-up longer experiment (10 week treatment) showed no effect on mechanics compared to untreated CKD animals (Allen et al., 2013; Moe et al., 2014). Neither study showed an effect (positive or negative) on cortical porosity compared to untreated CKD.

The results from these studies suggest that bisphosphonate treatment alone in CKD is insufficient to provide protection against bone fragility as the mechanical parameters were dominated by the effects of disease rather than bisphosphonate treatment. While bone mass is often seen as the critical factor to the mechanical integrity of bone, the distribution of material and its quality also play critical roles (Allen and Burr, 2007; Turner, 2002). Previous research has frequently captured the detrimental impacts of architecture and structural bone changes in CKD on structural- and estimated material-mechanical properties (Allen et al., 2013; Moe et al., 2014; McNerny et al., 2019; Newman et al., 2015). CKD drives changes beyond the macro and micro scale with CKD shown to lead to a greater accumulation of advanced glycation end products (AGE's) in both serum and bone which is thought to influence collagen cross-linking and the mineralization of bone (Chen et al., 2020; Allen et al., 2015). Additionally, it has been previously established that CKD can influence bone hydration (Allen et al., 2015) and the material composition of bone (Iwasaki et al., 2013; Iwasaki et al., 2011; Malluche et al., 2013). Therefore, this collection of prior research reaffirms the complexity of the disease and the number of variables that are changed and influence the biomechanical properties of bone in CKD.

Bisphosphonates have the potential to modify parameters that impact the bone tissue. Bisphosphonates have been highly effective in reducing fracture risk in post-menopausal osteoporosis due to improvements in bone mineral density (BMD) (Burr and Allen, 2012; Eastell et al., 2011). However, it has been noted that BMD only partially accounts for the reduction in fracture risk following bisphosphonate treatment (Pazianas et al., 2014). Creating low turnover states through bisphosphonate administration can have secondary consequences that include increasing the mean age of bone leading to an older matrix and bisphosphonates can alter the mineralization profile of bone (Pazianas et al., 2014; Allen and Burr, 2007). Acknowledging that CKD influences bone beyond quantity may be helpful in explaining why bisphosphonate treatment in this study was not able to recover mechanical properties as effectively as expected. Ideally, fracture-reduction therapies would improve bone mass and material properties; however, achieving this therapeutic combination is challenging and is unlikely to be achieved using bisphosphonates in CKD patients (Turner, 2002).

In both our studies, PTH was high in CKD animals which is hypothesized to be a driver of cortical porosity development. CKD animals treated with a single dose of zoledronate had higher cortical porosity compared to CKD animals treated with risedronate. Previously, we

hypothesized that high PTH leads to high osteocyte RANKL which, in turn, stimulates high osteoclastic drive to the cortical bone (Metzger et al., 2021a; Metzger et al., 2020a). In this study, we investigated whether the two bisphosphonate treatments in the adenine mice impacted osteocyte RANKL differently than CKD alone. Osteocytes positive for RANKL were higher in adenine vs. control as previously described (Metzger et al., 2021a; Metzger et al., 2020a) and both risedronate and zoledronate treatments resulted in 22–30% higher RANKL+ osteocytes than untreated adenine mice. Higher RANKL may partially explain the increase in cortical porosity in zoledronate-treated adenine mice but does not account for the similarly high RANKL values with lower porosity in the risedronate-treated groups. Therefore, it is likely that high PTH and high RANKL are not the sole drivers of cortical porosity in zoledronate-treated adenine mice. Thus, the mechanisms leading to higher cortical porosity with a single dose of zoledronate in CKD remains unclear at this time. Additionally, bone changes likely linked with high PTH and elevated osteocyte RANKL, indicate the potential need for combination treatments including both a PTH-lowering therapeutic, like calcimimetics, and an alternate anti-resorptive.

We acknowledge a few limitations to our study. First, the mechanism of delivery of zoledronate is not clinically transferable as we injected ZOL subcutaneously (SQ) in rats compared to the typical intravenous (IV) route in patients. However, our previous study showed that skeletal accumulation of zoledronate in rats is comparable between IV and SQ methods (Swallow et al., 2018). Additionally, zoledronate is not typically dosed in a fractionated pattern in patients, because its potency is such that only a single yearly injection is needed. However, to address this concern we used risedronate, a bisphosphonate with a dosing regimen that is more frequent. Third, experiment 1 was conducted in rats with a moderate stage of CKD (typically thought of as equivalent to late stage 3 or early stage 4); therefore, bone phenotypes that are typically associated with late-stage CKD, such as dramatic cortical porosity, were not present. However, this is also a strength as the rats earlier in the progression of the disease still had increased porosity with the single zoledronate dose indicating this type of dosing may not be beneficial at earlier disease stages. Additionally, comparisons of biochemical parameters between 10- and 14-week adenine mice show no differences between groups, indicating stable kidney disease in this timeframe. Due to this, we cannot speak to whether risedronate prevented an increase in porosity. Furthermore, rodent cortical bone differs in bone structure in comparison to human cortical bone. Since rodents lack osteons the results from this study should not be extrapolated to human bone without further investigation. Another limitation of this study is the use of different doses of bisphosphonate, different dosing durations, and different mechanical setups (3- vs. 4-point bending) in the two different rodent models. The variables were independently chosen for each model based on our past work, but we acknowledge that this limited direct comparison across the two experiments. Lastly, this study focused on the microstructure and mechanical impacts of bisphosphonates on cortical bone; therefore, analyses assessing the impacts of bisphosphonates on kidney function or specific molecular and cellular mechanisms contributing to higher rates of cortical porosity within bisphosphonate-treated groups are avenues of future investigation.

In conclusion, this study demonstrates that single dose zoledronate leads to higher cortical porosity compared to more frequent dosing of bisphosphonates (fractionated zoledronate or risedronate) in the setting of existing CKD. Bisphosphonate treatment demonstrated limited effectiveness in preventing microstructure cortical bone deterioration with mechanical parameters remaining compromised due to CKD irrespective of bisphosphonate treatment in animals with established disease. Future studies will likely need to utilize combination treatments to target the multiple mechanisms contributing to CKD-associated bone loss and compromised mechanical properties.

Supplementary data to this article can be found online at <https://doi.org/10.1016/j.bonr.2022.101174>.

CRedit authorship contribution statement

Elizabeth A. Swallow: Conceptualization, investigation, formal analysis, writing – original draft, writing – review & editing. **Corinne E. Metzger:** investigation, formal analysis, writing – review & editing. **Neal X. Chen:** Resources, writing & editing. **Joseph M. Wallace:** Resources, writing - editing & review. **Samantha P. Tippen:** investigation, writing – editing and reviewing. **Rachel Kohler:** methodology and investigation. **Sharon M. Moe:** Resources and Writing – editing and reviewing. **Matthew R. Allen:** Conceptualization, supervision, writing – review and editing, resources, and funding acquisition.

Declaration of competing interest

All authors declare that they have no conflicts of interest related to the presented work.

Acknowledgements

This work was supported by a United States (U.S.) Department of Veterans Affairs merit grant (BX003025) to MRA. The contents do not represent the views of the U.S. Department of Veterans Affairs or the United States Government.

References

- Alem, A.M., et al., 2000. Increased risk of hip fracture among patients with end-stage renal disease. *Kidney Int.* 58 (1), 396–399.
- Allen, M.R., Burr, D.B., 2007. Mineralization, microdamage, and matrix: how bisphosphonates influence material properties of bone. *BoneKEy-Osteovision* 4 (2), 49–60.
- Allen, M.R., Turek, J.J., Phipps, R.J., Burr, D.B., 2011. Greater magnitude of turnover suppression occurs earlier after treatment initiation with risedronate than alendronate. *Bone* 49 (1), 128–132.
- Allen, M.R., et al., 2013. Skeletal effects of zoledronic acid in an animal model of chronic kidney disease. *Osteoporos. Int.* 24 (4), 1471–1481.
- Allen, M.R., Newman, C.L., Chen, N., Granke, M., Jeffrey, S., Moe, S.M., 2015. Changes in skeletal collagen crosslinks and matrix hydration in high and low turnover chronic kidney disease. *Osteoporos. Int.* 26 (3), 977–985.
- Aref, M.W., McNerny, E.M.B., Brown, D., Jepsen, K.J., Allen, M.R., 2016. Zoledronate treatment has different effects in mouse strains with contrasting baseline bone mechanical phenotypes. *Osteoporos. Int.* 27 (12), 3637–3643.
- Ball, A.M., et al., 2002. Risk of hip fracture among dialysis and renal transplant recipients. *J. Am. Med. Assoc.* 288 (23), 3014–3018.
- Bergner, R., Henrich, D., Hoffmann, M., Schmidt-Gayk, H., Lenz, T., Uppenkamp, M., 2008. Treatment of reduced bone density with ibandronate in dialysis patients. *J. Nephrol.* 21 (4), 510–516.
- Berman, A.G., Clauser, C.A., Wunderlin, C., Hammond, M.A., Wallace, J.M., 2015. Structural and mechanical improvements to bone are strain dependent with axial compression of the tibia in female C57BL/6 mice. *PLoS One* 10 (6), 1–16.
- Bouxsein, M.L., Boyd, S.K., Christiansen, B.A., Guldberg, R.E., Jepsen, K.J., Müller, R., 2010. Guidelines for assessment of bone microstructure in rodents using micro-computed tomography. *J. Bone Miner. Res.* 25 (7), 1468–1486.
- Bowe, B., et al., 2018. Changes in the US burden of chronic kidney disease from 2002 to 2016: an analysis of the global burden of disease study. *JAMA Netw. Open* 1 (7).
- Burr, D.B., 2020. Fifty years of chronic bisphosphonates: what are their mechanical effects on bone? *Bone* 138 (May).
- Burr, D.B., Allen, M.R., 2012. Bisphosphonates and PTH for preventing fractures. In: Silva, M. (Ed.), *Skeletal Aging and Osteoporosis*, 5th ed. Springer, Berlin, Heidelberg. Center for Disease Control and Prevention, 2021. *Chronic Kidney Disease in the United States*, 2021. Atlanta, GA.
- Chen, N.X., et al., 2020. Effect of advanced glycation end-products (AGE) lowering drug ALT-711 on biochemical, vascular, and bone mass in a rat model of CKD-MBD. *J. Bone Miner. Res.* 35 (3), 608–617.
- Coco, M., Rush, H., 2000. Increased incidence of hip fractures in dialysis patients with low serum parathyroid hormone. *Am. J. Kidney Dis.* 36 (6), 1115–1121.
- Eastell, R., Walsh, J.S., Watts, N.B., Siris, E., 2011. Bisphosphonates for postmenopausal osteoporosis. *Bone* 49, 82–88.
- Ensrud, K.E., et al., 2007. Renal function and risk of hip and vertebral fractures in older women. *Arch. Intern. Med.* 167, 133–139.
- Fuchs, R.K., et al., 2008. Strontium ranelate does not stimulate bone formation in ovariectomized rats. *Osteoporos. Int.* 19 (9), 1331–1341.
- Iwasaki, Y., Kazama, J.J., Yamato, H., Fukagawa, M., 2011. Changes in chemical composition of cortical bone associated with bone fragility in rat model with chronic kidney disease. *Bone* 48 (6), 1260–1267.
- Iwasaki, Y., Kazama, J.J., Yamato, H., Shimoda, H., Fukagawa, M., 2013. Accumulated uremic toxins attenuate bone mechanical properties in rats with chronic kidney disease. *Bone* 57 (2), 477–483.

- Jokihaara, J., et al., 2008. Treatment of experimental renal osteodystrophy with pamidronate. *Kidney Int.* 74 (3), 319–327.
- Ketteler, M., et al., 2017. Executive summary of the 2017 KDIGO chronic kidney disease-mineral and bone disorder (CKD-MBD) guideline update: what's changed and why it matters. *Kidney Int.* 92 (1), 26–36.
- Kohler, R., et al., 2021. The effect of single versus group μ CT on the detection of trabecular and cortical disease phenotypes in mouse bones. *JBM Plus* 5 (4), 1–10.
- Lomashvili, K.A., Monier-Faugere, M.C., Wang, X., Malluche, H.H., O'Neill, W.C., 2009. Effect of bisphosphonates on vascular calcification and bone metabolism in experimental renal failure. *Kidney Int.* 75 (6), 617–625.
- Malluche, H.H., Porter, D.S., Pienkowski, D., 2013. Evaluating bone quality in patients with chronic kidney disease. *Nat. Rev. Nephrol.* 9 (11), 671–680.
- Mcnerney, E.M.B., Buening, D.T., Aref, M.W., Chen, N.X., Moe, S.M., Allen, M.R., 2019. Time course of rapid bone loss and cortical porosity formation observed by longitudinal μ CT in a rat model of CKD. *Bone* 125 (April), 16–24.
- Metzger, C.E., Swallow, E.A., Allen, M.R., 2020a. Elevations in cortical porosity occur prior to significant rise in serum parathyroid hormone in young female mice with adenine-induced CKD. *Calcif. Tissue Int.* 106 (4), 392–400.
- Metzger, C.E., et al., 2020b. Reversing cortical porosity: cortical pore infilling in preclinical models of chronic kidney disease. *Bone*.
- Metzger, C.E., Swallow, E.A., Stacy, A.J., Allen, M.R., 2021a. Strain-specific alterations in the skeletal response to adenine-induced chronic kidney disease are associated with differences in parathyroid hormone levels. *Bone* 148, 115963.
- Metzger, C.E., Swallow, E.A., Stacy, A.J., Allen, M.R., 2021b. Adenine-induced chronic kidney disease induces a similar skeletal phenotype in male and female C57BL/6 mice with more severe deficits in cortical bone properties of male mice. *PLoS One* 16 (4 April), 1–13.
- Moe, S.M., Nickolas, T.L., 2016. Fractures in patients with CKD: time for action. *Clin. J. Am. Soc. Nephrol.* 11, 1929–1931.
- Moe, S.M., et al., 2009. A rat model of chronic kidney disease-mineral bone disorder (CKD-BMD) and the effect of dietary protein source. *Vascular* 75 (2), 176–184.
- Moe, S.M., et al., 2011. The pathophysiology of early-stage chronic kidney disease-mineral bone disorder (CKD-MBD) and response to phosphate binders in the rat. *J. Bone Miner. Res.* 26 (11), 2672–2681.
- Moe, S.M., et al., 2014. A comparison of calcium to zoledronic acid for improvement of cortical bone in an animal model of CKD. *J. Bone Miner. Res.* 29 (4), 902–910.
- Newman, C.L., et al., 2014. Cortical bone mechanical properties are altered in an animal model of progressive chronic kidney disease. *PLoS One* 9 (6), 1–8.
- Newman, C.L., et al., 2015. Compromised vertebral structural and mechanical properties associated with progressive kidney disease and the effects of traditional pharmacological interventions. *Bone* 77, 50–56.
- Nickolas, T.L., McMahon, D.J., Shane, E., 2006. Relationship between moderate to severe kidney disease and hip fracture in the United States. *J. Am. Soc. Nephrol.* 17 (11), 3223–3232.
- Nickolas, T.L., Leonard, M.B., Shane, E., 2008. Chronic kidney disease and bone fracture: a rowing concern. *Kidney Int.* 74 (6), 721–731.
- Pazianas, M., van der Geest, S., Miller, P., 2014. Bisphosphonates and bone quality. *Bonekey Rep.* 3 (September 2013), 1–8.
- Russell, R.G.G., Watts, N.B., Ebetino, F.H., Rogers, M.J., 2008. Mechanisms of action of bisphosphonates: similarities and differences and their potential influence on clinical efficacy. *Int.* 19 (6), 733–759.
- Schaffler, M.B., Burr, D.B., 1988. Stiffness of compact bone: effects of porosity and density. *J. Biomech.* 21 (1), 13–16.
- Swallow, E.A., et al., 2018. Skeletal accumulation of fluorescently tagged zoledronate is higher in animals with early stage chronic kidney disease. *Osteoporos. Int.* 29 (9), 2139–2146.
- Swallow, E.A., et al., 2019. Skeletal levels of bisphosphonate in the setting of chronic kidney disease are independent of remodeling rate and lower with fractionated dosing. *Bone* 127 (July), 419–426.
- Tentori, F., et al., 2014. High rates of death and hospitalization follow bone fracture among hemodialysis patients. *Kidney Int.* 85 (1), 166–173.
- Toussaint, N.D., Lau, K.K., Strauss, B.J., Polkinghorne, K.R., Kerr, P.G., 2010. Effect of alendronate on vascular calcification in CKD stages 3 and 4: a pilot randomized controlled trial. *Am. J. Kidney Dis.* 56 (1), 57–68.
- Turner, C.H., 2002. Biomechanics of bone: determinants of skeletal fragility and bone quality. *Osteoporos. Int.* 13, 97–104.
- Turner, C.H., Burr, D.B., 1993. Basic biomechanical measurements of bone : a tutorial. *Bone* 14, 595–608.
- Wallace, J.M., Golcuk, K., Morris, M.D., Kohn, D.H., 2009. Inbred strain-specific response to biglycan deficiency in the cortical bone of C57BL6/129 and C3H/He mice. *J. Bone Miner. Res.* 24 (6), 1002–1012.
- Wilson, L.M., et al., 2017. Benefits and harms of osteoporosis medications in patients with chronic kidney disease: a systematic review and meta-analysis. *Ann. Intern. Med.* 166 (9), 649–658.